The Effect of Dynamic Interaction between Crude Oil and Low-Salinity Water on Asphaltene Instability: A Pore-Scale Perspective

Darya Saniei, Mohammad Hossein Behroozi, Hassan Mahani[a], Shahab Ayatollahi[a]

[1]Department of Chemical and Petroleum Engineering, Sharif University of Technology, Azadi Street, Tehran 11155-9465, Iran

[a] Authors to whom correspondence should be addressed:

shahab@sharif.edu

hmahani@sharif.edu

Abstract

Among enhanced oil recovery (EOR) methods, low-salinity waterflooding (LSWF) stands out as a practical and environmentally friendly approach. However, oil-brine incompatibility can cause asphaltene instability, precipitation, and likely formation damage. Due to the lack of published studies at the pore-scale, this work uniquely visualizes asphaltene precipitation during LSWF using a microfluidic technique, allowing real-time observation of oil-brine interactions and damage assessment. Transparent glass micromodels are utilized to simulate oil displacement near the wellbore. Real crude oil samples and various synthetic brines are tested to analyze the effects of asphaltene content and brine salinity on precipitation and deposition pattern. The findings reveal a direct correlation between crude oil asphaltene content and deposition. Lower salinity brines formed stable emulsions, increasing asphaltene deposition in swept zones. In contrast, unswept regions, such as dead-ends, experience lower deposition. This behavior can be attributed to the limited fluid dynamics in unswept regions, where low shear and restricted oil–water contact reduce the formation of emulsions and consequently asphaltene destabilization. Notably, two-times diluted Persian Gulf water (2DSW, ~23,800 ppm) led to 6.8% volumetric precipitation, compared to 5.1% for high-salinity formation brine (FW, ~189,000 ppm). Despite slightly higher deposition with low-salinity brines, the associated salinity change risks—such as plugging, flow impairment, and formation damage due to asphaltene deposition—are negligible under the studied conditions. This is a favorable outcome for deployment of LSWF. Moreover, the study highlights the critical role of brine composition and oil characteristics in LSWF, emphasizing the need for oil-brine compatibility assessment to mitigate any asphaltene-related damage and ensure effective recovery. These insights are essential for optimizing LSWF and minimizing formation damage risks in practical applications.

Keywords: Low-Salinity Waterflooding; Asphaltene Instability; Oil-Water Interface; Micromodel; Formation Damage

1. Introduction

After primary and secondary production, a significant amount of oil remains in the reservoir. Typically, primary recovery methods can extract about 20-30% of the original oil in place (OOIP), while secondary recovery methods, such as waterflooding—which are applied after the natural reservoir energy is depleted—can increase this to approximately 30–40% of OOIP. Enhanced Oil Recovery (EOR) techniques are then employed to target this remaining oil. EOR methods can potentially recover an additional 10-30% of the OOIP, depending on the specific method and reservoir conditions[1, 2]. Compared to other EOR methods, low-salinity waterflooding (LSWF) has been found to be effective in a wide range of oil reservoirs with varying crude oil compositions and rock types [3-5]. Research by Mahani et al. [6] highlights the role of

wettability alteration as a critical effect of LSWF, particularly in carbonate reservoirs, where ionic composition plays a significant role in oil recovery. Moreover, recent comprehensive reviews, such as the work of Mahani and Thyne (2023) [7] , have further reinforced LSWF's efficacy, especially in oil-wet to mixed-wet carbonate reservoirs, by focusing on its ability to improve sweep efficiency and accelerate oil recovery through ionic interaction optimization. In this regard, Afekare and Radonjic [8] emphasized that LSWF mechanisms are scale-dependent and require integrated evaluation from nano-scale interactions up to reservoir-scale simulations. Consistent with these observations, Al-Attar et al. [9] experimentally demonstrated that adjusting brine salinity and sulfate concentration in carbonate cores substantially alters wettability and can improve recovery by more than 20% in optimized LSWF scenarios.

Evaluation of the possible damages due to LSWF is strictly necessary before the injection stage. One of the most concerning challenges, which is referred to in several studies, is asphaltene precipitation/deposition in emulsified systems [8, 10-14]. Microfluidic investigations have shown that ionic content, emulsion morphology, and the physicochemical properties of the oil-brine interface directly impact asphaltene precipitation patterns and severity [15].

Recent studies have further elucidated the physicochemical mechanisms governing asphaltene instability under enhanced oil recovery (EOR) conditions. Mahdavi and Saeedi Dehaghani [16] demonstrated that the combination of smart water and clay particles significantly destabilizes asphaltene molecules, leading to emulsion formation. Abdi et al. [17] revealed that reductions in interfacial tension due to ion exchange mechanisms directly influence the aggregation dynamics of asphaltenes. Similarly, Hamidian et al. [18] found that binary salt mixtures significantly affect the oil–brine interfacial behavior, while Shadervan et al. [19] investigated the role of surface-modified nanoparticles in delaying asphaltene precipitation and enhancing oil recovery.

Recent findings suggest that the presence of specific ions in the aqueous phase plays a vital role in destabilizing asphaltenes at the oil–brine interface, thereby influencing both emulsion stability and the extent of deposition [20]. Moreover, studies using micromodel visualization have shown that lower salinity conditions generally lead to enhanced asphaltene instability, whereas higher salinity helps maintain asphaltene stability in the oil phase [10]. Moreover, Several reviews emphasize that while SARA-based indicators offer quick predictions, dynamic deposition analysis at pore-scale provides a more accurate assessment of instability, especially under EOR conditions [21].

Our recent studies have provided insights into the intricate relationship between rock types and brine salinity during LSWF. Salari et al. (2024) [22] emphasized that the presence of calcite rock significantly enhances asphaltene precipitation compared to quartz, particularly in emulsified systems with diluted Persian Gulf seawater. This is in-line with newer experimental studies that demonstrate how high-valence ions like Fe^{3+} significantly influence droplet size and emulsion stability, thus altering asphaltene distribution across oil sub-fractions [23].

Complementing these findings, Mokhtari et al. [24] conducted a detailed investigation into fluid-fluid interactions, demonstrating that reduced brine salinity increases the dissolution of crude oil's polar components into the aqueous phase. Ali et al. [21] also demonstrated that changes in polar component solubility and SARA fractions could be used to optimize injection strategies and predict flocculation risks. They also confirmed that the presence of low-salinity water alters the chemical properties of the effluent brine, underlining the significance of optimizing salinity levels for effective EOR techniques [24]. Additionally, recent studies show that molecular structure—such as the dominance of island vs. archipelago motifs—can strongly influence aggregation behavior, indicating that oil source and thermal maturity are key considerations in modeling asphaltene stability [15].

Furthermore, Balavi et al. [25] explored the simultaneous effects of calcite particles and brine salinity on asphaltene stability. Their research identified an intermediate salinity range where asphaltene instability peaks

due to increased adsorption at the oil/brine interface. This phenomenon was further supported by UV-Vis spectroscopy and zeta-potential measurements, which revealed stronger electrostatic interactions between calcite and asphaltene at higher salinities. These insights are critical for designing LSWF strategies that minimize formation damage while maximizing oil recovery.

Unlike the overwhelming number of papers on fluid−fluid interactions as the underlying mechanisms of LSWF, only a few research works have been published on investigation of the negative side effects of LSWF such as asphaltene instability, emulsion formation, and organic scaling. These effects eventually impede the flow behavior and formation damage [26-29]. The traditional works on asphaltene precipitation and deposition are mostly focused on the oil reservoir depletion during primary production or the gas injection as the secondary or tertiary recovery stages [29-31] where asphaltene can be destabilized due to pressure reduction or incompatibility of the injection gas with the crude oil (reduction of their solubility in oil). Among a few research works on water-oil interaction, the study by Shojaati et. al. investigated the emulsion phenomenon on asphaltene precipitation. They concluded that at low and moderate salt concentrations, asphaltene instability increases and asphaltene accumulates more at the oil/brine interface leading to the asphaltene precipitation and deposition [32]. Also, Mokhtari et. al. [33] reported that asphaltene stability is reduced after LSWF due to the interaction between the organic phase and low-salinity water at the reservoir condition. experimental works do not resemble the basic concept of LSWF in asphaltic oil reservoirs as they have utilized synthetic model oil samples and the dynamic test scenarios are limited.

In view of the deficiencies in the published papers and open questions, the main objective and novelty of this study is to visually investigate asphaltene precipitation using real reservoir oil samples and realistic brine compositions (based on the ionic composition of formation water) in a heterogeneous microfluidic system. Two oil samples taken from two middle-eastern oil reservoirs with high and low asphaltene contents were chosen as the oleic phase. Besides, high- and low-salinity brine samples with different salt concentrations are utilized to fully investigate the interaction of phases for asphaltene instability assessment during co-injection of oil and brine. The micromodel structure utilized here is already tested and its potential to visualize solid precipitation was verified by Mirkhoshhal et.al [34]. Finally, by applying high-resolution digital imaging, a deeper and more quantitative pore-scale analysis of emulsion formation and asphaltene precipitation are obtained.

2. Materials and Methods

A microfluidic setup made of a high-resolution digital microscope, and a fabricated porous micromodel is used in this laboratory work to investigate asphaltene precipitation due to LSWF. To assess the relationship between the injection brine salinity and its effects on emulsion formation and asphaltene precipitation, different oil samples and brines were tested. Using image analysis enabled us to obtain the average percentage of asphaltene precipitation for different oil-brine mixtures. More detailed explanation of the materials and methods used in this study are provided in the following sections.

2.1. Fluids

2.1.1. Oil Samples

In this study, two distinct oil samples from separate Iranian oil reservoirs were utilized to explore asphaltene precipitation and emulsion formation. Table 1 presents the significant differences in physical properties and chemical composition of these two oil samples, notably their asphaltene content. n-C5 (normal pentane) was used as the asphaltene precipitant in all related measurements. Additionally, asphaltene instability coefficients were calculated for both oils using two commonly applied formulas: Stability Index (SI) (Eq. 1) and Colloidal

Instability Index (CII) (Eq. 2). These coefficients provide valuable insights into the stability of asphaltenes within each oil sample.

$$SI = \frac{Aspahltene\ (wt\%)}{Resins\ (wt\%)} \quad \text{Eq.1}$$

$$CII = \frac{Aspahltene\ (wt\%) + Saturates\ (wt\%)}{Resins\ (wt\%) + Aromatic\ (wt\%)} \quad \text{Eq.2}$$

As shown in Table 2, oil sample A demonstrates overall stability based on the formulas, while oil sample B exhibits general instability, indicating a higher likelihood of asphaltene precipitation and flow assurance challenges. However, these indices have been developed for primary depletion or gas injection [35]. Their suitability for water injection is debatable and should be only used as a primary indication.

2.1.2. Brine Samples

Two types of brine were used in this study: formation water (FW) and twice-diluted Persian Gulf seawater (2DSW). These brines were selected based on previous studies and experiences on low-salinity waterflooding in our research group. The brines were prepared by dissolving the precise quantities of salts in deionized (DI) water and were mixed using a magnetic heater stirrer (Alpha; D500). Also, six different types of salts (all with laboratory purity exceeding 99%) were purchased from Dr. Mojalali Chemical Company. The salt concentrations for all aqueous phases are detailed in Table 3.

2.1.3. Solvents

In this study, laboratory-grade normal pentane (n-C5) with a purity exceeding 99%, and toluene with a purity exceeding 99%, supplied by BioChem, were used to induce asphaltene instability within the micromodel.

2.2. Micromodel Fabrication and Characterization

The porous medium used in this study was a transparent, double-sided glass micromodel and was fabricated as follows. A heterogeneous porous medium was drawn using CorelDRAW software and a bitmap image was produced. The bitmap image was then transferred onto a borosilicate glass plate using a CO_2 laser ablation system (Universal Laser Systems, model PLS6.75), while the other glass plate was left blank. The two glass plates were fused in a programmable laboratory furnace at 670˚C for 4 hours, and then gradually cool to 25˚C to prevent any thermal cracking. A schematic of the micromodel is shown in Figure 1, where the dark-colored regions represent flow paths such as pores, the inlet, and outlet channels, and the bright regions denote the grains. The physical characteristics of the micromodel are present in Table 4. Prior to the experiments, the micromodel was verified to be water-wet through standard pre-saturation and flow pattern observation. No chemical treatment was applied to alter the surface wettability.

2.3. Experimental set-ups and procedures

2.3.1. Experimental set-ups

As illustrated in Figure 2, the microfluidic setup is composed of three main elements: 1) the injection pumps, 2) the porous micromodel, and 3) the imaging and data processing system. A high precision syringe pump (LongerPump TS2-60) was used for brine and oil injection. A Dino-Lite microscope (model MC-1600x) with adjustable magnification up to 1000x was used for capturing real-time images. An LED backlight source

was used for the illumination of the micromodel and capturing optimal images of fluid flow in the porous medium. The recorded images were then post-processed using ImageJ®.

2.4. Experimental procedure

The dynamic micromodel experiments conducted in this study were designed to directly observe and quantify asphaltene deposition resulting from the interactions between brine and crude oil. All experiments were carried out at ambient temperature and pressure, using procedure outlined below:

1. To avoid air entrapment in the micromodel, at least 4 pore volumes (PVs) of carbon dioxide were injected, as CO_2 partially dissolves in water and enhances full saturation during subsequent brine injection.
2. The micromodel was then flooded with dyed formation water, using a water-soluble food-grade dye (from Khat-e-Zard company, to displace CO_2 and fully saturate the micromodel. At least 4 PVs (pore volumes) of formation water were injected. At this step the porosity and pore volume of the micromodel were determined.
3. 8 PVs of a 50%-50% target brine-crude oil mixture were simultaneously injected into the micromodel at a rate of 1.8 mL/h to saturate the porous medium. This approach was adopted to create a uniform saturation and ensure sufficient interaction between oil and brine within the limited observation area of the micromodel. It allows for more controlled and observable emulsion formation and asphaltene behavior under dynamic conditions.
4. 15 PVs n-pentane were injected into the micromodel to induce asphaltene instability in the porous medium. In this step, asphaltene deposition occurred in different regions of the micromodel in different extents.
5. Finally, for visualization and quantification of the deposited asphaltene, digital images were taken to compare with those at the initial condition. The average precipitated asphaltene was calculated using ImageJ® software, based on determining the asphaltene precipitated area divided by the lateral area of the pore space.

The test procedure is shown schematically in Figure 3. Images were taken at two different time periods: before and after n-pentane injection. Although no histogram of asphaltene size distribution was extracted, all imaging was performed at fixed locations in the micromodel to allow for temporal comparisons before and after precipitation. All images were taken from the emulsified sections, as these regions are the most probable sites for asphaltene deposition. The target regions were then categorized into two sections: “low-emulsified” and “highly-emulsified” regions. The terms "low-emulsified" and "highly-emulsified" used in this paper refer to regions with relatively less and more water-in-oil emulsions, respectively. After converting the images to grayscale for better distinction by the software, the average precipitated asphaltene was calculated. Although a detailed droplet size distribution analysis was not performed, visual differentiation of highly- and low-emulsified regions was conducted using optical inspection and grayscale image analysis.

3. Design of Experiments

As four types of fluids (two oil samples and two brines) were used in this study, four distinct microfluidic experiments were designed to visualize and quantify asphaltene deposition due to contact with low- and high-salinity water. The designed experiments are represented in Table 5. The salinity values (TDS in ppm) of FW and 2DSW are provided in Table 3.

4. Results and Discussion

The interfacial interaction between low-salinity water/crude oil can generate in-situ water-in-oil emulsions driven by asphaltene stabilizing action as surfactant at the oil/water interface. The presence of asphaltene molecules in crude oil may increase the energy needed to break these emulsions, which can inhibit oil recovery and increase the oil production cost [36-38]. Using both visual and quantitative approaches described in the previous section, the study aimed to address the relationship between emulsion formation and asphaltene precipitation/deposition and brine salinity. Figure 4 provides an example of both regions observed after injection of 8 PVs of oil-brine and 15 PVs of n-pentane. In Figure 4a, a "highly-emulsified" region of the pore space where more water-in-oil emulsions and larger water blobs are observed in the investigation area. In Figure 4b, a "low-emulsified" region with relatively low water-in-oil emulsion and finer water blobs are observed. The highly-emulsified regions are located in flowing areas where there is a high flow velocity leading to the agitation of water-oil mixture, leading to the formation of emulsions. In contrast, low-emulsified regions are located in low-flow areas, dead-ends and by-passed areas. In such regions, the limited oil–brine interaction and minimal shear stress suppress emulsion formation, resulting in less asphaltene destabilization and precipitation.

The differences between high-salinity water and low-salinity water are evident in the behavior of asphaltene precipitation and emulsion stability. Low-salinity water (2DSW, ~23,800 ppm) injections result in a higher degree of asphaltene precipitation, particularly in highly emulsified regions, due to increased interfacial activity and salinity-induced destabilization of asphaltenes. In comparison, high-salinity water (FW, ~189,000 ppm) stabilizes asphaltenes by maintaining a lower interfacial activity and reducing emulsion formation. These differences arise because high salinity provides ions that mitigate asphaltene aggregation, while low salinity alters ionic balance, enhancing water-oil interactions and promoting precipitation.

Figure 5 shows the pore-scale images of the emulsified and low-emulsified regions of the micromodel after the simultaneous injection of crude oil A and each brine sample followed by normal pentane injection. Images (a) and (b) correspond to the highly-emulsified and low-emulsified regions, respectively. Images (c) and (d) represent the corresponding regions after the injection of oil sample A and twice distilled Persian Gulf seawater (2DSW). The encircled areas highlight the deposited asphaltene resulting from normal pentane injection. The deposition is significantly more pronounced in the low-salinity water experiments, further corroborating the destabilizing effect of reduced salinity on asphaltene stability. In certain observations such as in Figure 5a, the irregular asphaltene accumulation may be attributed to local variations in pore geometry, flow dynamics, or uneven emulsion distribution, all of which can influence interfacial interactions. While not fully quantified in this study, these anomalies merit further investigation.

Figure 6 shows four zoomed-in pore-scale images of the experiments conducted with oil sample B, which, according to Table 1, differs significantly from oil sample A, particularly in terms of asphaltene composition percentage. As illustrated in Figure 6, the effect of water-in-oil emulsions and salinity on asphaltene precipitation and deposition is more pronounced when the amount of dissolved asphaltene in the crude oil composition is higher. This result highlights the crucial role of crude oil composition in pore-scale studies.

Based on the literature and the observations made in this study (Figures 5 and 6), the emulsification of water in the crude oil phase makes asphaltene molecules more unstable, leading to their precipitation [12, 22, 39]. As seen in both Figures 5 and 6, the highly-emulsified regions contain more deposited asphaltene than the low-emulsified regions. Another key finding from these tests is that asphaltene precipitation and deposition generally occur more frequently with low-salinity brine injection. This phenomenon can be attributed to the ionic imbalance created by low-salinity water, which disrupts the stability of the asphaltene molecules in the crude oil. Low-salinity water reduces the concentration of divalent cations (such as calcium and magnesium) that stabilize asphaltene particles in suspension, leading to an increase in interfacial activity and the aggregation of asphaltenes at the water-oil interface. Additionally, the increased interfacial activity enhances emulsification, which further destabilizes asphaltenes and promotes their precipitation and deposition.

The pore-scale behavior of oils A and B reveals significant differences in asphaltene precipitation and deposition under low-salinity water injection. Oil A, with a relatively lower asphaltene content, shows less extensive precipitation and deposition across both highly-emulsified and low-emulsified regions. In contrast, oil B, with a higher asphaltene content, exhibits more widespread and pronounced asphaltene deposition, particularly in highly emulsified regions where interfacial activity is heightened. The differences can be attributed to the compositional variation between the two oils. Oil B's elevated asphaltene levels make it more sensitive to destabilizing factors such as ionic imbalance and increased emulsification, leading to higher aggregation and deposition. Furthermore, the significantly higher resin content in oil B may enhance initial asphaltene dispersion but also increase the likelihood of interfacial adsorption and bridging under salinity-induced stress, contributing to greater instability. This emphasizes the critical role of crude oil composition in determining the response to low-salinity water injection at the pore scale. These results highlight that even oils with relatively low asphaltene mass percentages are at risk of precipitation, underscoring the importance of evaluating asphaltene behavior to manage precipitation risks effectively.

Figure 7 presents a grayscale image of the micromodel taken after the injection of n-pentane, which followed the injection of formation water and the oil-low salinity brine mixture using oil sample A. The black dots in the image indicate asphaltene precipitation, as asphaltene molecules are among the least reflective components in the oil phase.

Figure 8 presents a grayscale image taken from the micromodel during tests conducted with oil sample B. Due to the higher asphaltene content in this oil sample, a greater accumulation of deposited asphaltene is observed, indicated by the black dots. The circled regions in each image highlight areas of asphaltene precipitation and deposition. These occupied areas were used to calculate the average asphaltene precipitation percentage.

The average precipitated asphaltene for each test was quantified, and the results are presented in Figure 9 as a bar chart (For clarity, ER refers to Emulsified Region and LER refers to Low-Emulsified Region.). The data indicate that the highest percentage of precipitated asphaltene was observed in tests conducted with oil sample B, which had the highest dissolved asphaltene content according to its SARA analysis. Additionally, the low-salinity water injection with 2DSW resulted in a higher percentage of asphaltene deposition.

Figure 10 presents the overall average asphaltene precipitation quantified after each brine phase injection. The results indicate that low-salinity water injection significantly impacts asphaltene precipitation and deposition in both crude oils A and B, despite their compositional differences. However, compared to the formation water, the differences are minimal. These findings corroborate the results of a recent study by Salari et al. (2024), which utilized the same oil and brine phases. The study demonstrated that interfacial tension (IFT) values are minimized in 2DSW brine, leading to increased instability and higher asphaltene precipitation [22].

Figure 11 provides a visual representation of the results presented in Figures 9 and 10. As illustrated, the percentage of precipitated asphaltene shows a clear relationship with both emulsion formation and brine salinity, which is referred to as fluid/fluid interaction in the literature. The outcomes that indicate asphaltene agglomeration and precipitation for the cases with higher emulsion content. The results of this study align with the findings of a other published research works in this area [25, 40, 41].

Besides, it was shown that the precipitated asphaltenes accumulate more in the corners and small throats because of their affinity to attach to the surface of micromodel. This would be more challenging if the porous rock is tight, heterogenic with more rough surfaces. More studies are ongoing to assess these parameters on possible damage result in from this phenomenon during LSWF in asphaltic oil reservoirs.

Investigations into the influence of oil type and emulsion quantity yielded significant insights into asphaltene deposition dynamics. A direct correlation is observed between the concentration of asphaltenes in the oil and the extent of asphaltene deposition, where a higher asphaltene content leads to increased deposition amount. As shown in Figure 9, oil sample B (10.6 wt.% asphaltene) exhibited an average deposition percentage approximately twice that of oil A (1.5 wt.%), quantitatively supporting the observed correlation. This

underscores the pivotal role of asphaltene concentration in dictating deposition behavior, as higher concentrations provide a greater pool of asphaltene molecules available for aggregation and deposition. Moreover, studies examining the relationship between asphaltene deposition and emulsion quantity reveal a direct relationship, with larger quantities of emulsion resulting in heightened deposition rates. Although the floc size was not directly measured, visual observations suggested that in low-asphaltene oil (sample A), larger isolated deposits occasionally formed, possibly due to insufficient resin content to maintain colloidal dispersion. This may result in fewer but larger flocs compared to oil B, where finer but more widespread deposition was observed. This phenomenon is attributed to the increased interfacial area between water and oil phases in places with emulsion content, which facilitates greater contact and promotes asphaltene aggregation and subsequent deposition.

Conclusions

This study investigates asphaltene precipitation and deposition as influenced by emulsion formation and brine salinity through microfluidic experiments. These micromodel tests offer a valuable intermediate approach between static and bulk tests and the more complex and costly core flood experiments. By utilizing image processing techniques for precise quantification, this research has provided several critical insights into the phenomena of asphaltene deposition. The primary conclusions drawn from the study are as follows:

- Pore-scale images reveal that asphaltene molecules were more unstable in regions with a higher possibility of emulsion formation. This finding highlights the role of water-in-oil emulsions in enhancing asphaltene precipitation and deposition, a conclusion that was further substantiated by the quantification of the acquired images.
- Furthermore, even with oils of relatively low asphaltene mass percentages (e.g., less than 2% in some cases), distinct dark-colored regions indicative of asphaltene deposition were observed. This low asphaltene mass percentage might seem insignificant, but even small amounts can destabilize under specific conditions, such as low-salinity water injection, due to ionic disruptions and enhanced interfacial activity.
- Our investigations also revealed that the composition of injected water impacts asphaltene deposition. Specifically, deviations from formation water, such as the injection of twice-diluted Persian Gulf seawater (2DSW), resulted in somewhat more asphaltene deposition compared to the formation water. This effect was particularly evident with certain oil samples, emphasizing the crucial role of water chemistry in asphaltene deposition dynamics and its implications for reservoir management practices. Nevertheless, the areal coverage of the deposited asphaltene between high-salinity and low-salinity cases differs between 1-2% which means that the risk of increased asphaltene instability with low-salinity brine is slightly higher. It is noteworthy that we used normal pentane – as a stimulator - which can result in the maximum possible asphaltene deposition. It is expected that under more natural deposition conditions, the amount of deposited asphaltene would be much less.

The insights gained from this study emphasize the need for reservoir engineers to incorporate asphaltene stability considerations into their management practices. Understanding how emulsion formation and water chemistry influence asphaltene deposition can lead to more effective strategies for preventing and mitigating asphaltene-related problems in oil reservoirs. Looking ahead, several promising avenues for future research could further elucidate asphaltene deposition dynamics. Exploring additional types of crude oil and brines, including synthetic oils and engineered brines, may provide deeper insights into asphaltene behavior and contribute to the development of more effective mitigation strategies.

Acknowledgments

The authors are grateful to Mrs. Armaghan Karimi and Mr. Amirhossein Salari, for their assistance in performing the experiments and preparing the image analysis.

References

1. Hasan, M.M., *Various techniques for enhanced oil recovery: A review.* Iraqi Journal of Oil & Gas Research, 2021. **2**(1).https://doi.org/10.55699/ijogr.2022.0201.1018
2. Thomas, S., *Enhanced oil recovery-an overview.* Oil & Gas Science and Technology-Revue de l'IFP, 2008. **63**(1): p. 9-19.https://doi.org/10.2516/ogst:2007060
3. Rostami, P., et al., *Effect of water salinity on oil/brine interfacial behaviour during low salinity waterflooding: A mechanistic study.* Petroleum, 2019. **5**(4): p. 367-374.https://doi.org/10.1016/j.petlm.2019.03.005
4. Al-Shalabi, E.W. and K. Sepehrnoori, *A comprehensive review of low salinity/engineered water injections and their applications in sandstone and carbonate rocks.* Journal of Petroleum Science and Engineering, 2016. **139**: p. 137-161.https://doi.org/10.1016/j.petrol.2015.11.027
5. Lager, A., et al., *Low salinity oil recovery-an experimental investigation1.* Petrophysics-The SPWLA Journal of Formation Evaluation and Reservoir Description, 2008. **49**(01).
6. Mahani, H., et al., *Insights into the mechanism of wettability alteration by low-salinity flooding (LSF) in carbonates.* Energy & Fuels, 2015. **29**(3): p. 1352-1367. 1352-1367, https://doi.org/10.1021/ef5023847
7. Mahani, H. and G. Thyne, *Low-salinity (enhanced) waterflooding in carbonate reservoirs*, in *Recovery Improvement*. 2023, Elsevier. p. 39-107.39-107, https://doi.org/10.1016/B978-0-12-823363-4.00007-8
8. Afekare, D.A. and M. Radonjic, *From mineral surfaces and coreflood experiments to reservoir implementations: Comprehensive review of low-salinity water flooding (LSWF).* Energy & fuels, 2017. **31**(12): p. 13043-13062.https://doi.org/10.1021/acs.energyfuels.7b02730
9. Al-Attar, H.H., et al. *Low salinity flooding in a selected carbonate reservoir: experimental approach*. in *SPE Europec featured at EAGE Conference and Exhibition?* 2013. SPE. https://doi.org/10.2118/164788-MS
10. Siadatifar, S.E., M. Fatemi, and M. Masihi, *Pore scale visualization of fluid-fluid and rock-fluid interactions during low-salinity waterflooding in carbonate and sandstone representing micromodels.* Journal of Petroleum Science and Engineering, 2021. **198**: p. 108156.https://doi.org/10.1016/j.petrol.2020.108156
11. Soleymanzadeh, A., et al., *Theoretical and experimental investigation of effect of salinity and asphaltene on IFT of brine and live oil samples.* Journal of Petroleum Exploration and Production, 2021. **11**: p. 769-781.https://doi.org/10.1007/s13202-020-01020-1
12. Salehpour, M., et al., *Contribution of water-in-oil emulsion formation and pressure fluctuations to low salinity waterflooding of asphaltic oils: A pore-scale perspective.* Journal of Petroleum Science and Engineering, 2021. **203**: p. 108597.https://doi.org/10.1016/j.petrol.2021.108597
13. Darvish Sarvestani, A., S. Ayatollahi, and M. Bahari Moghaddam, *Smart water flooding performance in carbonate reservoirs: an experimental approach for tertiary oil recovery.* Journal of Petroleum Exploration and Production Technology, 2019. **9**(4): p. 2643-2657.https://doi.org/10.1007/s13202-019-0650-9
14. Amirian, T., M. Haghighi, and P. Mostaghimi, *Pore scale visualization of low salinity water flooding as an enhanced oil recovery method.* Energy & Fuels, 2017. **31**(12): p. 13133-13143.https://doi.org/10.1021/acs.energyfuels.7b01702
15. Punase, A., et al. *Microscale Evaluation of Asphaltene Deposition to Comprehend its Instability Mechanism*. in *SPE International Conference on Oilfield Chemistry*. 2025. SPE.
16. Mahdavi, M.S. and A.H.S. Dehaghani, *Experimental study on the simultaneous effect of smart water and clay particles on the stability of asphaltene molecule and emulsion phase.* Scientific Reports, 2025. **15**(1): p. 3393. 3393, https://doi.org/10.1038/s41598-025-87821-y
17. Abdi, A., et al., *Investigating the mechanism of interfacial tension reduction through the combination of low-salinity water and bacteria.* Scientific Reports, 2024. **14**(1): p. 11408. 11408, https://doi.org/10.1038/s41598-024-62255-0

18. Hamidian, R., M. Lashkarbolooki, and A.Z. Hezave, *Interfacial tension and contact angle of asphaltenic and resinous model oil in the presence of binary salts mixtures.* Scientific Reports, 2024. **14**(1): p. 18018. 18018, https://doi.org/10.1038/s41598-024-68740-w
19. Shadervan, A., et al., *Mechanistic understanding of asphaltene precipitation and oil recovery enhancement using SiO2 and CaCO3 nano-inhibitors.* Scientific Reports, 2024. **14**(1): p. 15249. 15249, https://doi.org/10.1038/s41598-024-65995-1
20. Mahdavi, S. and A. Mousavi Moghadam, *Critical review of underlying mechanisms of interactions of asphaltenes with oil and aqueous phases in the presence of ions.* Energy & Fuels, 2021. **35**(23): p. 19211-19247. 19211-19247, https://doi.org/10.1021/acs.energyfuels.1c02270
21. Ali, S.I., et al., *Critical analysis of different techniques used to screen asphaltene stability in crude oils.* Fuel, 2021. **299**: p. 120874. 120874, https://doi.org/10.1016/j.fuel.2021.120874
22. Salari, A., et al., *Water/oil emulsion and asphaltene instability in different formations during low-salinity waterflooding: an experimental study.* Scientia Iranica, 2024. 10.24200/sci.2024.63830.8615
23. Shahsavani, B., M. Riazi, and M.R. Malayeri, *Asphaltene instability in the presence of emulsified aqueous phase.* Fuel, 2021. **305**: p. 121528. 121528, https://doi.org/10.1016/j.fuel.2021.121528
24. Mokhtari, R., S. Ayatollahi, and M. Fatemi, *Experimental investigation of the influence of fluid-fluid interactions on oil recovery during low salinity water flooding.* Journal of Petroleum Science and Engineering, 2019. **182**: p. 106194. 106194, https://doi.org/10.1016/j.petrol.2019.106194
25. Balavi, A., S. Ayatollahi, and H. Mahani, *The simultaneous effect of brine salinity and dispersed carbonate particles on asphaltene and emulsion stability.* Energy & Fuels, 2023. **37**(8): p. 5827-5840. 5827-5840, https://doi.org/10.1021/acs.energyfuels.3c00293
26. Ghasemian, J., et al., *Effect of salinity and ion type on formation damage due to inorganic scale deposition and introducing optimum salinity.* Journal of Petroleum Science and Engineering, 2019. **177**: p. 270-281. 270-281, https://doi.org/10.1016/j.petrol.2019.02.019
27. Rezaei, N. and A. Firoozabadi, *Macro-and microscale waterflooding performances of crudes which form w/o emulsions upon mixing with brines.* Energy & fuels, 2014. **28**(3): p. 2092-2103. 2092-2103, https://doi.org/10.1021/ef402223d
28. Alagic, E. and A. Skauge, *Combined low salinity brine injection and surfactant flooding in mixed− wet sandstone cores.* Energy & fuels, 2010. **24**(6): p. 3551-3559. 3551-3559, https://doi.org/10.1021/ef1000908
29. Akbarzadeh, K., et al., *Asphaltenes—problematic but rich in potential.* Oilfield review, 2007. **19**(2): p. 22-43. 22-43,
30. Andersen, S.I. and K.S. Birdi, *Influence of temperature and solvent on the precipitation of asphaltenes.* Petroleum Science and Technology, 1990. **8**(6): p. 593-615. 593-615, https://doi.org/10.1080/08843759008915946
31. Ali, S.I., et al., *Factorial analysis of experimental parameters effecting asphaltene precipitation in dead crude oils.* Arabian Journal for Science and Engineering, 2023. **48**(7): p. 9519-9533. 9519-9533, https://doi.org/10.1007/s13369-023-07702-2
32. Shojaati, F., et al., *Investigating the effect of salinity on the behavior of asphaltene precipitation in the presence of emulsified water.* Industrial & Engineering Chemistry Research, 2017. **56**(48): p. 14362-14368. 14362-14368, https://doi.org/10.1021/acs.iecr.7b03331
33. Mokhtari, R., et al., *Asphaltene destabilization in the presence of an aqueous phase: The effects of salinity, ion type, and contact time.* Journal of Petroleum Science and Engineering, 2022. **208**: p. 109757. 109757, https://doi.org/10.1016/j.petrol.2021.109757
34. Mirkhoshhal, S.M., et al., *Pore-scale insights into sludge formation damage during acid stimulation and its underlying mechanisms.* Journal of Petroleum Science and Engineering, 2021. **196**: p. 107679. 107679, https://doi.org/10.1016/j.petrol.2020.107679
35. Guzmán, R., et al., *Methods for determining asphaltene stability in crude oils.* Fuel, 2017. **188**: p. 530-543. 530-543, https://doi.org/10.1016/j.fuel.2016.10.012
36. Masalmeh, S., et al. *Low salinity water flooding in carbonate: screening, laboratory quantification and field implementation*. in *Abu Dhabi International Petroleum Exhibition and Conference*. 2019. SPE. https://doi.org/10.2118/197314-MS
37. Emadi, A. and M. Sohrabi. *Visual investigation of low salinity waterflooding*. in *International symposium of the society of core analysts, Aberdeen, Scotland, UK*. 2012.

38. Mahzari, P. and M. Sohrabi. *Crude oil/brine interactions and spontaneous formation of micro-dispersions in low salinity water injection*. in *SPE Improved Oil Recovery Conference?* 2014. SPE. https://doi.org/10.2118/169081-MS
39. Fingas, M., *Water-in-oil emulsion formation: A review of physics and mathematical modelling.* Spill Science & Technology Bulletin, 1995. **2**(1): p. 55-59. 55-59, https://doi.org/10.1016/1353-2561(95)94483-Z
40. Tetteh, J.T. and R. Barati, *Crude-oil/brine interaction as a recovery mechanism for low-salinity waterflooding of carbonate reservoirs.* SPE Reservoir Evaluation & Engineering, 2019. **22**(03): p. 877-896. 877-896, https://doi.org/10.2118/194006-PA
41. Ayirala, S., et al., *Multiscale aqueous-ion interactions at interfaces for enhanced understanding of controlled-ionic-composition-waterflooding processes in carbonates.* SPE Reservoir Evaluation & Engineering, 2020. **23**(03): p. 1118-1132. 1118-1132, https://doi.org/10.2118/199343-PA

List of Tables and Figures

Table1. Properties of crude oil samples.

Oil Sample	Viscosity(cP) @ 25˚C	API (˚)	Saturates(wt.%)	Aromatic (wt.%)	Resins (wt.%)	Asphaltenes (wt.%)
A	2.2	35	70.5	20.5	7.5	1.5
B	4.3	22.3	33.3	42.3	13.9	10.6

Table2. Asphaltene Instability Coefficients for Oil Samples A and B.

Stability Parameters		Stability Index (SI)	Colloidal Instability Index (CII)
Oil Sample	A	0.2 (Stable)	2.57 (Unstable)
	B	0.76 (Unstable)	0.78 (Stable)
Stability Assessment	-	SI ≥ 2: Stable SI < 2: Unstable	CII < 1: Stable CII ≥ Unstable

Table3. The salt concentration of brine samples.

Salt/Brine type	**FW**	**2DSW**
NaCl	154.031	12.788
KCl	1.193	0.559
$CaCl_2.2H_2O$	24.11	0.882
$MgCl_2.6H_2O$	8.933	5.9975
Na_2SO_4	0.426	3.409
$NaHCO_3$	0.672	0.168
Total Dissolved Solids: TDS (ppm)	189,365	23,803
pH	6.7	8.0

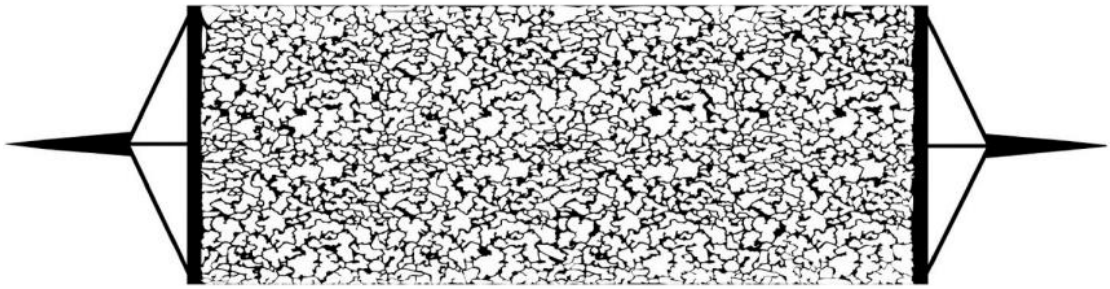

Figure 1 Schematic of the micromodel pattern

Table4. The physical characteristics of the micromodels used in the flow experiments

Length (cm)	Width (cm)	Pore volume (cc)	Pore throat diameter (µm)	Etched depth (µm)	Porosity (%)	Coordination number
16.5	6	0.37	100-200	160	34.6	3-4

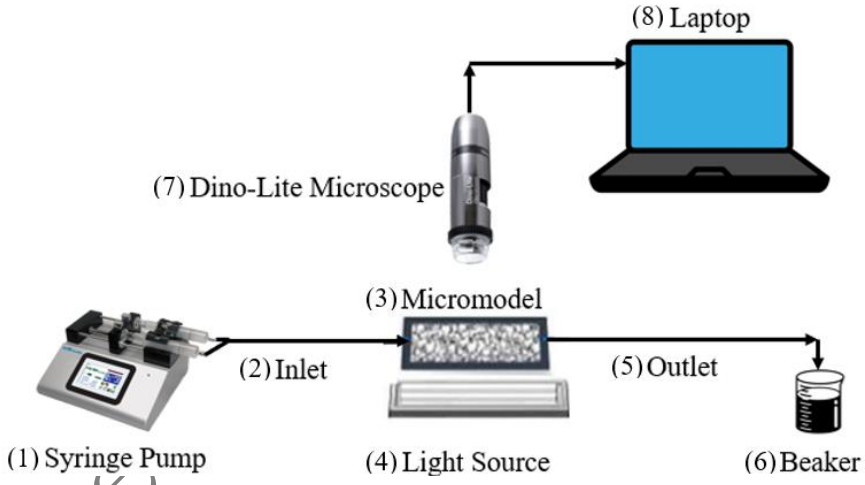

Figure 2 Schematic of the microfluidic system and its elements: (1) High-precision syringe pump, (2) Inlet, (3) Porous Micromodel, (4) Light source, (5) Outlet, (6) Beaker for collecting the exiting fluid, (7) Dino-Lite microscope, (8) Personal computer for data and image acquisition and processing.

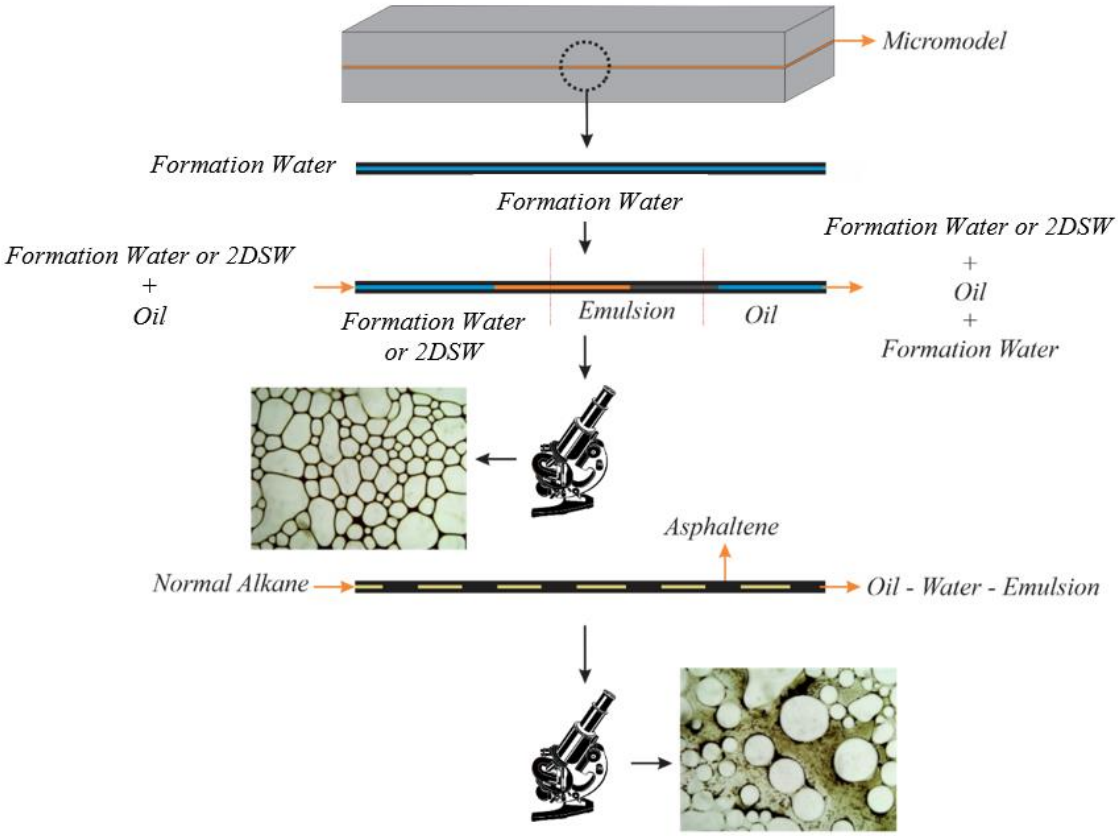

Figure 3 Procedure of the dynamic experiments with the micromodel

Table5. Design of microfluidic experiments

#	Brine Sample	Oil Sample	Objective
1	Formation water (FW)	A	A base case for comparison between low-saline and formation water (FW)
2	Twice-diluted Persian Gulf water (2DSW)	A	Effect of low-salinity water (2TDW) on asphaltene precipitation/deposition with low-asphaltene content oil
3	Formation water (FW)	B	A base case for comparison between low saline and formation water (FW)
4	Twice-diluted Persian Gulf water (2DSW)	B	Effect of low-salinity water (2TDW) on asphaltene precipitation/deposition with high-asphaltene content oil

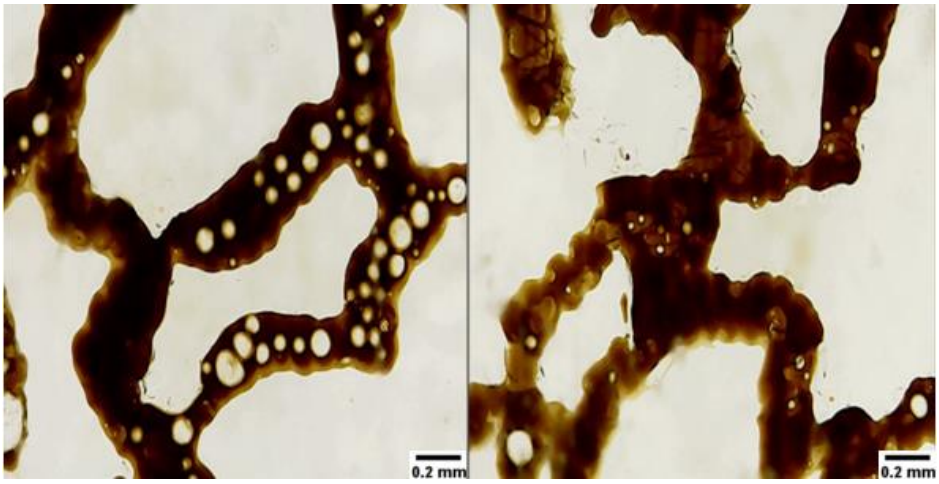

a b

Figure 4: a) Highly-emulsified and b) Low-emulsified regions in the micromodel during test with oil A and formation water (FW). Images captured after 8 PVs of oil-brine injection and 15 PVs of n-C5 flushing. Flow rate: 1.8 mL/h. Conditions: ambient temperature and pressure.

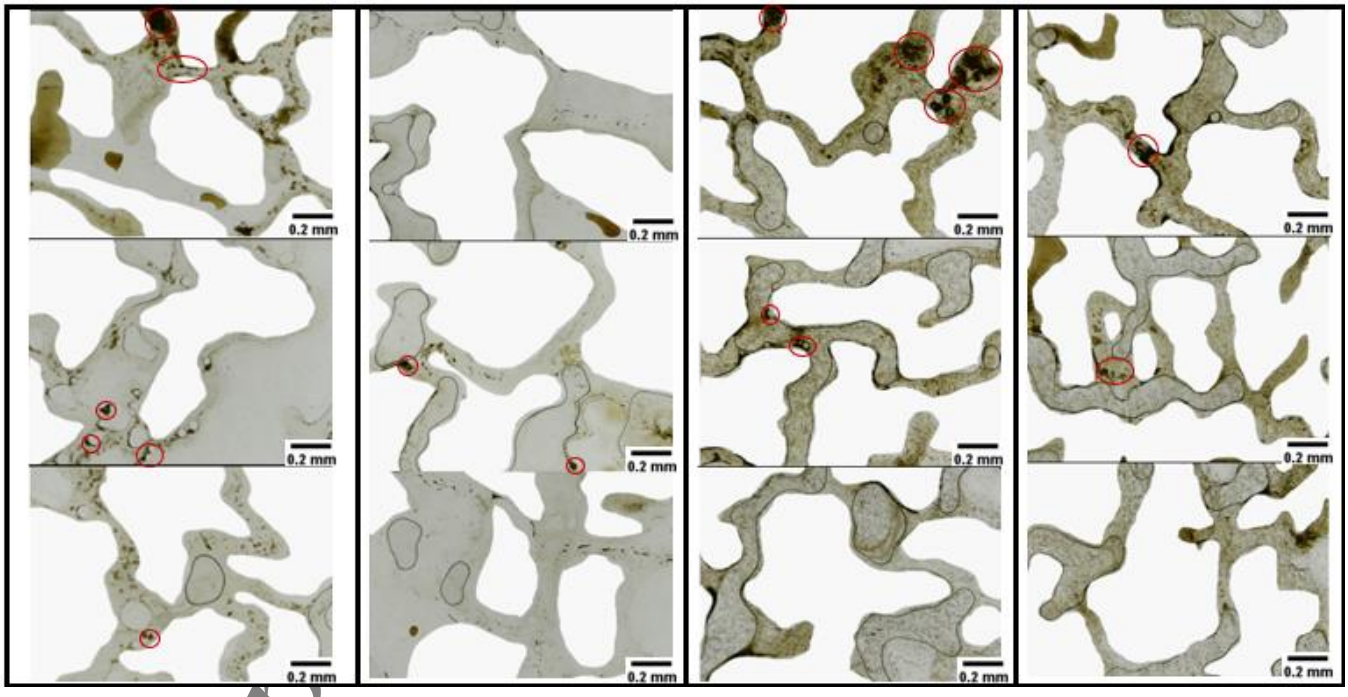

a b c d

Figure 5.Pore-scale images of the emulsified and low-emulsified regions of the micromodel after the simultaneous injection of crude oil A and each brine sample .Images (a) and (b) are tests with formation water (FW, ~189,000 ppm), and images (c) and (d) are with twice-diluted Persian Gulf water (2DSW, ~23,800 ppm).Additionally, (a) and (c) represent highly-emulsified regions, whereas (b) and (d) correspond to low-emulsified regions. All images were taken after injecting 8 PVs of oil-brine mixture at 1.8 mL/h followed by 15 PVs of n-C5. Test conditions: ambient temperature and pressure.

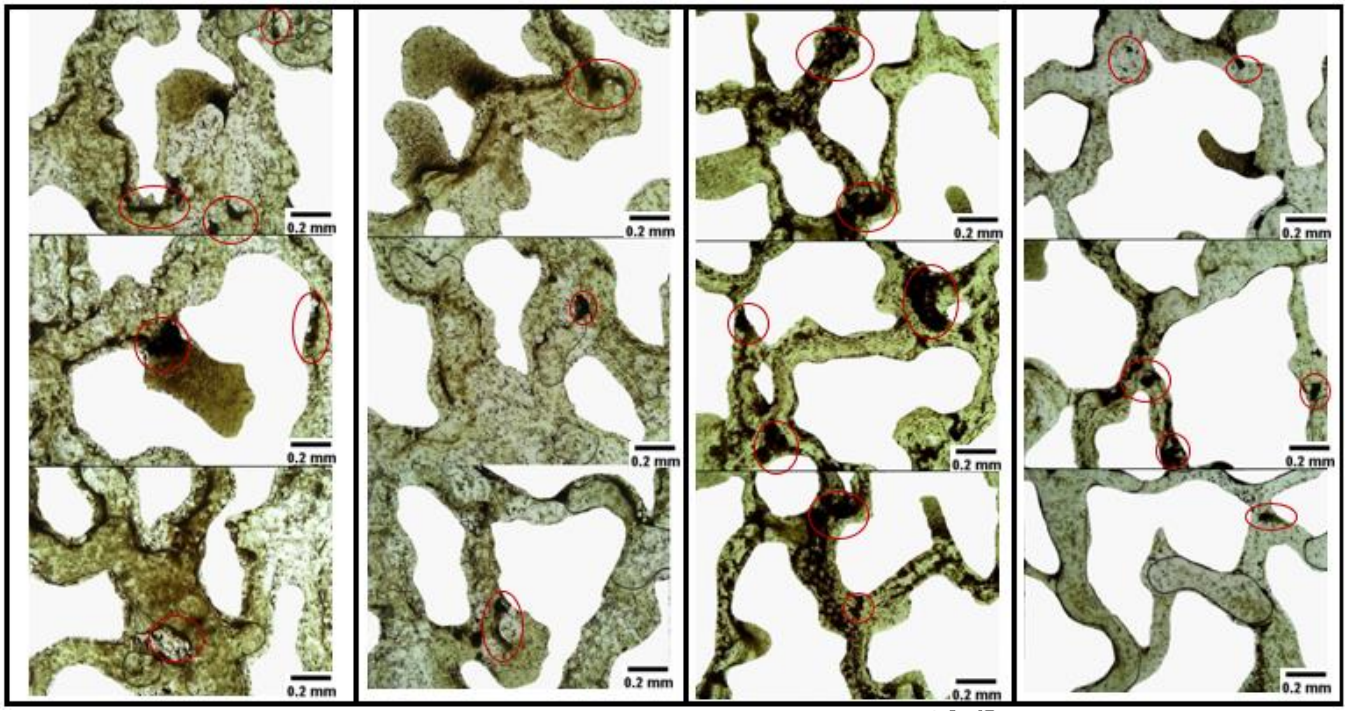

a b c d

Figure 6. Zoomed-in pore-scale images of the experiments conducted with oil sample B. Images (a) and (b) are tests with FW, and images (c) and (d) are with 2DSW. (a) and (c) show highly-emulsified regions; (b) and (d) show low-emulsified regions. Captured after 8 PVs of oil-brine co-injection and 15 PVs of n-C5. Test conditions: ambient pressure and temperature.

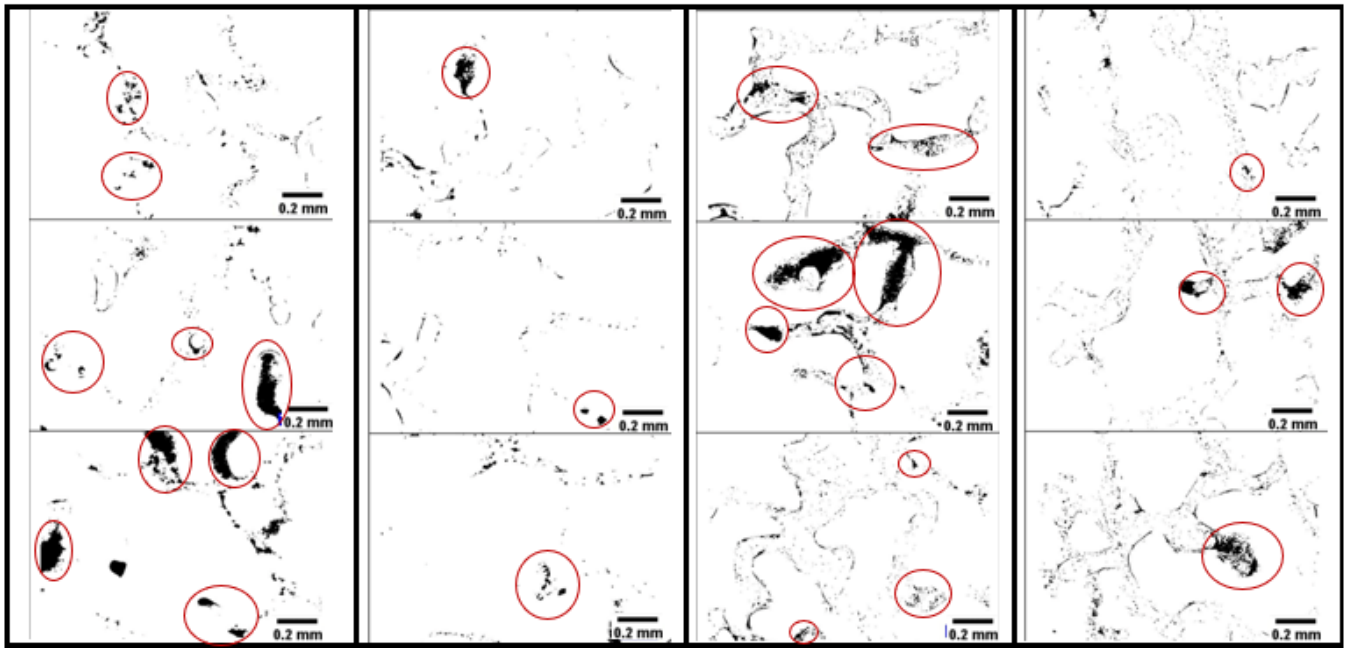

a b c d

Figure 7 Grayscale pore-scale images from micromodel tests with oil sample A after FW and 2DSW injections. Images (a), (b): FW; images (c), (d): 2DSW. (a), (c): highly-emulsified zones; (b), (d): low-emulsified zones. Images taken after 8 PVs brine-oil co-injection and 15 PVs of normal pentane. Conditions: 1.8 mL/h, ambient pressure and temperature.

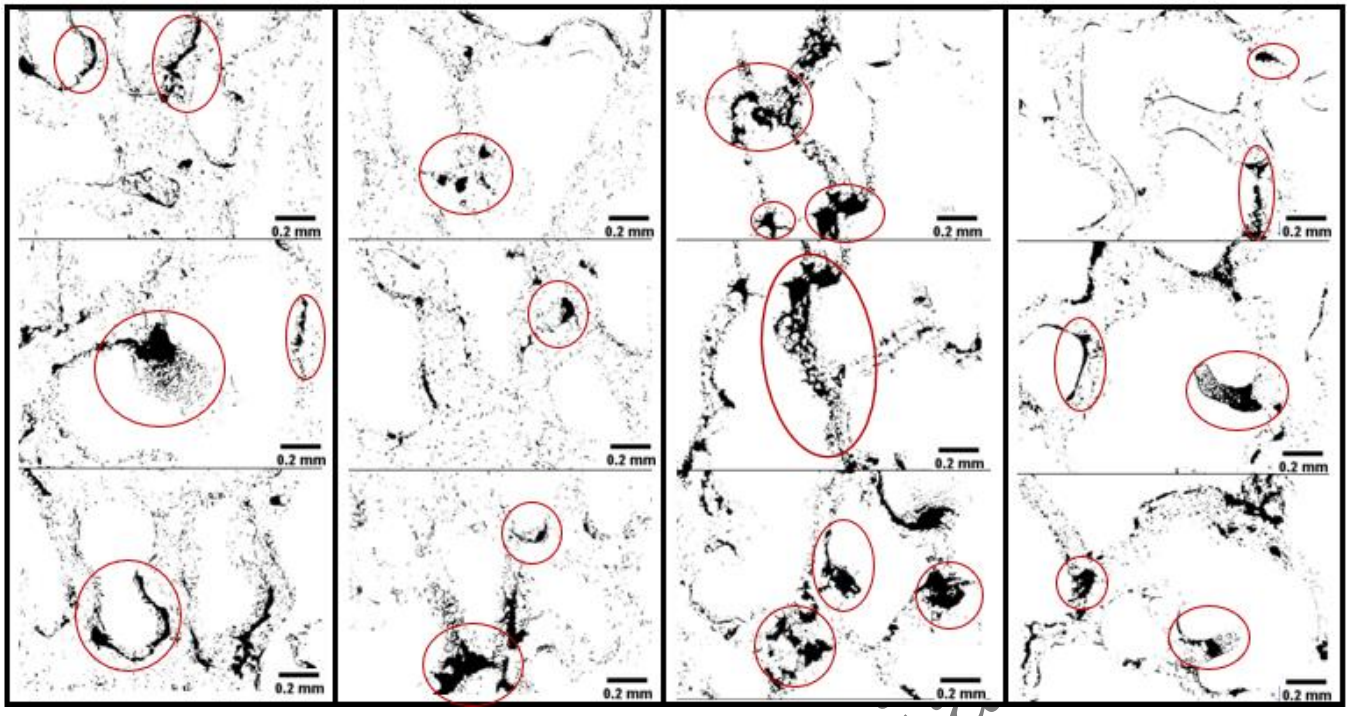

Figure 8 Grayscale images from micromodel tests with oil B. Higher accumulation of asphaltene deposits observed due to higher asphaltene content. Images (a), (b): FW; (c), (d): 2DSW. (a), (c): emulsified; (b), (d): low-emulsified. Captured after 8 PVs of oil-brine injection and 15 PVs of n-C5 at 1.8 mL/h.

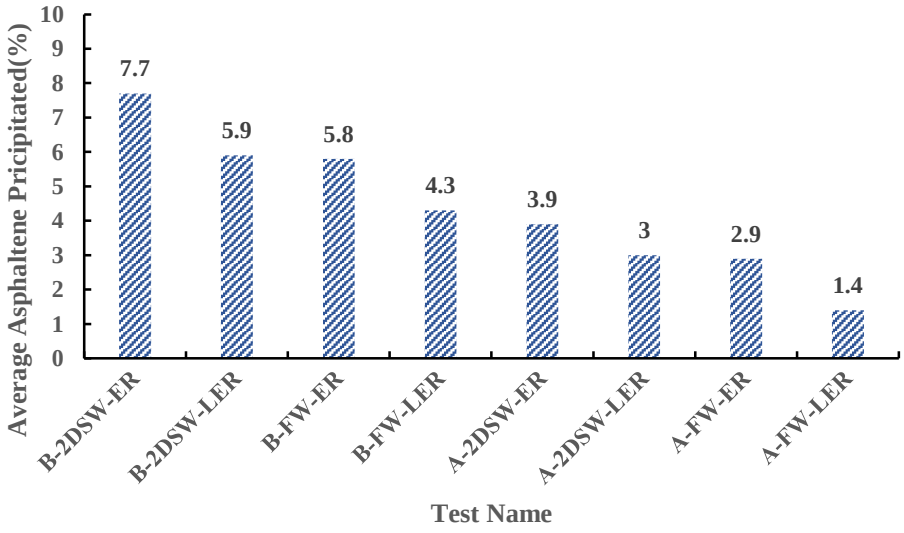

Figure 9 Average asphaltene precipitation in oil samples A and B with both 2DSW and FW(ER: Emulsified Region; LER: Low-Emulsified Region). Results based on image analysis after injecting 8 PVs oil-brine mixture + 15 PVs n-C5.

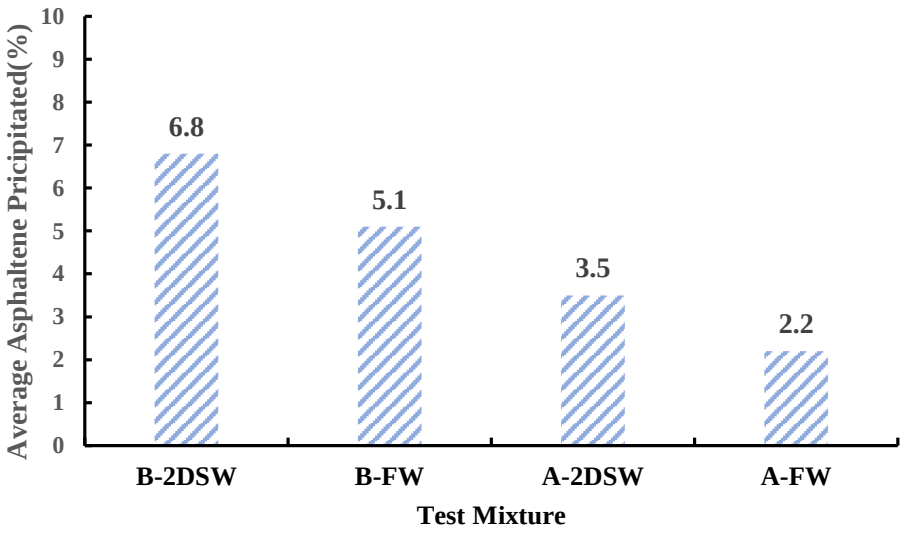

Figure 10 Overall average asphaltene precipitation in oil samples A and B with different brines. Conditions: 8 PVs oil-brine + 15 PVs pentane injection; ambient conditions; flow rate: 1.8 mL/h.

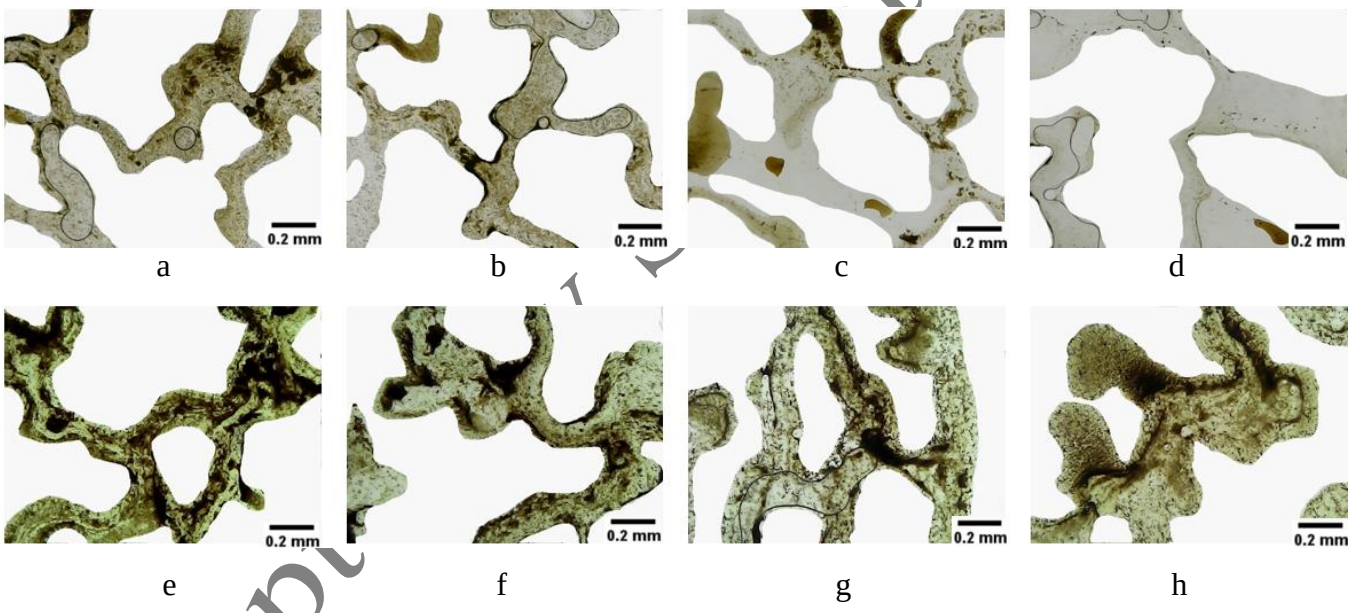

Figure 11 Visual comparison of asphaltene deposition across all experimental runs. (a–d): oil A; (e–h): oil B. 2DSW in (a, b, e, f); FW in (c, d, g, h). Highly-emulsified zones: (a, c, e, g); low-emulsified: (b, d, f, h). Images taken post 8 PVs oil-brine and 15 PVs n-C5 injection.

Authors' Biographies

Shahab Ayatollahi is a Professor in the Department of Chemical and Petroleum Engineering at Sharif University of Technology in Tehran. He earned both his BSc and MSc degrees in Chemical Engineering from Shiraz University, and obtained his PhD in Chemical Engineering from the University of Waterloo, Canada, in 1995. He has authored over three hundred publications in the field of oil reservoir engineering. His leading research focuses on enhanced oil recovery (EOR) from tight and asphaltenic reservoirs, pore structure, rock-fluid and fluid-fluid interactions, and multiphase flow in porous media.

Hassan Mahani is an Associate Professor of Petroleum Engineering at Sharif University of Technology. He earned his PhD in Petroleum Engineering from Imperial College London and his MSc in Chemical Engineering from Sharif University of Technology. Before joining Sharif University, he worked as a principal investigator and scientist at Shell Technology Centers in the Netherlands. He currently serves as an Associate Editor for SPE Journal and Geoenergy Science and Engineering Journal. His research is centered on the fundamental understanding, quantitative evaluation, modeling, and prediction of multiphase flow in porous media, with applications in improved and enhanced oil recovery (IOR/EOR), geoengineering, and environmental studies. His current work focuses on water-based and low-salinity EOR, underground hydrogen and energy storage, contaminant gas storage, pore-scale physics and digital rocks, as well as geochemistry and geomechanics.

Darya Saniei is currently a Master's student of Reservoir Engineering at Sharif University of Technology, since 2023. She obtained her bachelor's degree in Petroleum Engineering at Sharif University of Technology in 2023. Her research interests include enhanced oil recovery from hydrocarbon reservoirs and fluid–rock interactions.

Mohammad Hossein Behroozi completed his bachelor's degree in Petroleum Engineering at the Petroleum University of Technology in 2021. He obtained his MSc degree in Reservoir Engineering at Sharif University of Technology in 2025. His areas of expertise include enhanced oil recovery and risk assessment of injection processes.